The Monte Carlo Method: Versatility Unbounded In A Dynamic Computing World
Chattanooga, Tennessee, April 17–21, 2005, on CD-ROM, American Nuclear Society, LaGrange Park, IL (2005)

CLINICAL BRACHYTHERAPY DOSIMETRY PARAMETERS AND MIXED-FIELD DOSIMETRY FOR A HIGH DOSE RATE Cf-252 BRACHYTHERAPY SOURCE

Christopher S. Melhus and Mark J. Rivard
Department of Radiation Oncology
Tufts – New England Medical Center
Boston, MA 02111
cmelhus@tufts-nemc.org; mrivard@tufts-nemc.org

Bernadette L. Kirk and Luiz C. Leal
Radiation Safety Information Computational Center
Oak Ridge National Laboratory
Oak Ridge, TN 37831
blk@ornl.gov; e5a@ornl.gov

ABSTRACT

Since the early 1970's, thousands of patients have been treated worldwide using low dose rate (LDR) californium-252 brachytherapy sources. With recent advances in radiochemistry for concentrating the radionuclide and increasing the effective specific activity, there is now potential for fabrication of high dose rate (HDR) ^{252}Cf brachytherapy sources. Consequently, the mixed-field radiation dose distributions from this novel source type must be characterized preceding delivery of patient treatments. Towards clinical implementation of HDR ^{252}Cf brachytherapy at Tufts-New England Medical Center, the mixed-field dosimetry for this source type has been examined using Monte Carlo methods (MCNP5) and compared to dose distributions produced by traditional HDR ^{192}Ir brachytherapy sources and other medically acceptable sources. The mixed-field dose distribution in the vicinity of a proposed HDR ^{252}Cf brachytherapy source was calculated in a spherical phantom composed of water. The ^{252}Cf neutron energy spectrum was modeled using the ENDF7205 energy spectrum as currently recommended by NIST. The ^{252}Cf photon energy spectrum was modeled using the bare ^{252}Cf source spectrum as measured by Skarsvåg *et al*. (Phys Rev C, 1980). The source capsule was composed of a Pt/Ir-10% alloy, with the radioactive source modeled as a cylindrical Pd wire. A ^{252}Cf source active length of 5.0 mm was used. The MCNP F4 and F6 (track length estimate of energy flux and deposition, respectively) calculation tallies were utilized for determining various dosimetric components. These include the source photon, neutron capture photon, and fast neutron dose components. Calculations were performed in a polar coordinate system to readily permit conversion of dose distribution results into the AAPM TG-43U1 dosimetry formalism for extracting clinical dosimetry parameters. Using this dosimetry formalism, results indicated that dosimetry parameters for HDR ^{252}Cf sources did not significantly differ from those determined for LDR ^{252}Cf sources. These data may now be integrated into brachytherapy treatment planning software to permit clinical implementation of HDR ^{252}Cf brachytherapy.

Key Words: Californium-252, brachytherapy dosimetry parameters

1 INTRODUCTION

In the first proposed medical application of ^{252}Cf brachytherapy, a preliminary 1D dose distribution was shown comparing the estimated localized dose deposition from an implanted source to that expected from an external collimated beam.[1] Although the figure clearly demonstrated sparing of healthy tissue through administering interstitial or intracavity radiation therapy, the figure could not be utilized towards implementing treatment planning of ^{252}Cf brachytherapy. Many authors subsequently improved upon the 1D characterization using experimental and calculative techniques to either determine the transverse plane dose or compute an *along-and-away* dose rate table. Anderson collected and compared the results of nine publications in 1973, and recommended the data of Colvett *et al.* (1972) for describing the applicator tube type source, an LDR source design.[2]

Although Anderson noted that additional dosimetry measurements were warranted, few studies of ^{252}Cf brachytherapy dosimetry parameters were published until the 1992 Yanch and Zamenhof Monte Carlo study in support of boron neutron capture therapy, which presented *along-and-away* dose rate tables.[3] The American Association of Physicists in Medicine (AAPM) Task Group No. 43 report (TG-43), published in 1995, established a factorized, polar coordinate system for representing the dose distribution about a brachytherapy source.[4] The TG-43 dosimetry formalism improved the accuracy of reproducing dose distributions towards clinical implementation, compared to 2D interpolations between data points on an *along-and-away* table. The TG-43 formalism also provided a means for evaluating similar brachytherapy source designs through direct comparison of the different parameters, *e.g.*, radial dose function g(r) or anisotropy function ϕ_{an} (r). Rivard *et al.* (1999) first applied the TG-43 methodology to the neutron absorbed dose from an LDR ^{252}Cf applicator tube type source.[5]

TG-43 was recently evaluated and updated (TG-43U1).[6] The updated report was limited to ^{103}Pd and ^{125}I sources due to uncertainties involved in applying the methodology to high-energy and/or mixed-field radiations. In this study, the TG-43U1 methodology was applied to the neutron and photon radiations from a theoretical HDR ^{252}Cf source.

2 MATERIALS AND METHODS

2.1 Monte Carlo Source Model Geometry

The HDR ^{252}Cf source is shown in **Figure 1**. A right cylinder with an active length L = 5.00 mm and a radius of 0.39 mm was used as the source volume. Although sources manufactured at Oak Ridge National Laboratory (ORNL) are in the from of a Pd:Cf_2O_3 cermet rod, the source material was modeled solely as Pd.[7] For a 2 mg source strength, *i.e.*, 2 mg of ^{252}Cf, the cermet wire is approximately 7% ^{252}Cf by mass. The source was contained in a cylindrical Pt/Ir-10% capsule with an outer length of 8.80 mm and outer radius of 0.648 mm. An air gap between the source element and capsule was not included, and the theoretical capsule was in contact with the source in all directions.

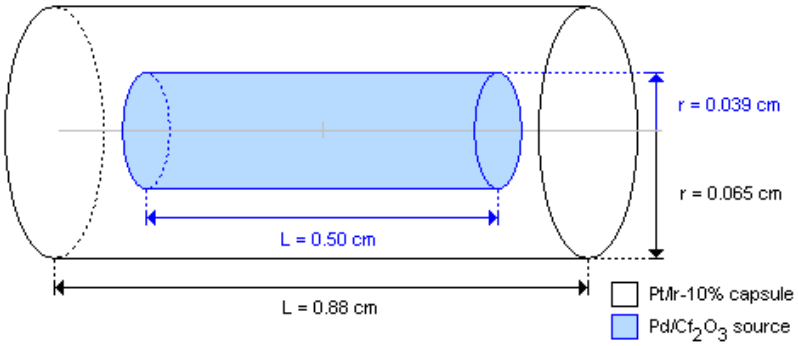

Figure 1. Schematic of theoretical HDR ^{252}Cf source modeled in this study.

The theoretical source was positioned in the center of a 50 cm diameter water phantom. Assuming standard temperature and pressure, a mass density of 0.998 g cm^{-3} for water was applied, and the S(α,β) thermal neutron scattering library LWTR.60t was selected. **Table I** shows the elemental composition and density of the materials used in this study, in addition to the photon and neutron cross section libraries called.

Table I. The MCNP5 cross section library called for neutrons and photons (n / p) and the nuclide mass composition of the three materials included in the simulations.

Nuclide	Libraries n / p	Material		
		H_2O	$Pd\text{-}Cf_2O_3$	Pt/Ir-10%
^{1}H	66c / p04	11.19	-	-
^{16}O	66c / p04	88.81	-	-
^{106}Pd	66c / p04	-	100.00	-
^{191}Ir	66c / p04	-	-	3.73
^{193}Ir	66c / p04	-	-	6.27
Pt	42c / p04	-	-	90.00
	ρ [g cm^{-3}]	0.998	12.0	21.505

2.2 Monte Carlo Tally Types and Simulation Defaults

Version 5 of the Monte Carlo N-Particle Transport Code System (MCNP5) was used to perform radiation transport calculations.[8] Two separate simulations were performed to assess the dose distribution from neutrons and photons emitted by ^{252}Cf. The first used MODE N P to determine the dose from neutrons and from photons induced through neutron transport as a result of capture or inelastic scattering, hereafter called "secondary" photons. The second set of simulations used MODE P to predict the dose distribution from photons emitted directly from ^{252}Cf, referred to as "primary" photons.

For both MODE N P and MODE P calculations, the track length estimate of cell-heating tally (F6) was employed to determine the energy deposited in the cell in units of MeV g^{-1} per source particle. In addition, at 11 radial distances between 0.75 and 17.5 cm, F6 and F4 (track-length estimator [cm^{-2}]), tallies were calculated at 38 energies between 0 and 20 MeV for neutrons, and F6, F4, and *F4 (track-length estimator of energy flux [MeV cm^{-2}]) tallies were

determined at 0.05 MeV increments between 0 and 8.35 MeV for primary and secondary photons.

For neutron transport, comparison of F6 and F4 results were evaluated to ensure that energy deposition closely matched neutron kerma coefficients published by the International Commission on Radiation Units and Measurement (ICRU) in Report 63.[9] Photon transport results were similarly appraised by comparing the ratio of F6 and *F4 results to the appropriate mass-energy attenuation coefficient published by the National Institute of Standards and Technology (NIST).[9]

Photo-nuclear physics (PHYS:P) was not incorporated because (γ,n) cross-sections for the materials in **Table I** are negligible below 10 MeV.[10] Preliminary analyses were performed using 10^8 histories for MODE N P neutron transport equations and 10^9 histories for MODE P primary photon transport. Variance reduction techniques were not employed.

2.3 ^{252}Cf Radiation Spectrum

Spontaneous fission of ^{252}Cf occurs in 3.092% of disintegrations, and results in the emission of 2.314 x 10^9 neutrons s^{-1} mg^{-1} and 1.320 x 10^{10} photons s^{-1} mg^{-1}. The neutron energy spectrum was modeled using data measured by Mannhart and published in the Evaluated Nuclear Data Files (ENDF/B-VI) by the Cross Section Evaluation Working Group at Brookhaven National Laboratory in 1991.[10,11]

Photon energy spectra were modeled using data published by Skarsvåg (1980) for energies between 0.114 and 2.54 MeV and Verbinski *et al.* (1973) for energies between 2.54 and 8.5 MeV.[12,13] The Skarsvåg-Verbinski data comprises 23 energy bins between 0 and 8.5 MeV, but does not include delayed emissions from the relaxation of fission products. Additional Monte Carlo simulations were performed using values recommended by Knauer *et al.* (1991).[14] The Knauer *et al.* spectrum includes thirteen 0.5 MeV energy bins between 0 and 6.5 MeV, and nearly 50% of the photons are emitted by fission products below 2.0 MeV. The average energy is 0.72 and 0.77 MeV for the Skarsvåg-Verbinski and Knauer *et al.* spectra, respectively.

The ENDF do not include data for photon radiation from ^{252}Cf. Additional measurements of ^{252}Cf photon radiation are needed to improve accuracy and consistency of future computational studies.

2.4 Dosimetry Methodology

The TG-43U1 protocol for the calculation of brachytherapy dosimetry parameters was followed, including the nine specifications for reporting Monte Carlo methodology. Both 1D and 2D parameters were determined for a theoretical encapsulated HDR ^{252}Cf source. While the protocol includes only low-energy photon-emitting radionuclides, the methodology was applied towards describing the mixed-field dose distribution about a ^{252}Cf source. Similar utilization of the original Task Group No. 43 methodology has been made by Rivard *et al.* and by Rivard for low-dose rate ^{252}Cf neutron dosimetry.[4,15]

The dosimetry parameters g(r), F(r,θ), and ϕ_{an}(r) were determined using a polar coordinate sampling space similar to that described by Rivard *et al.*[16] Radial sampling at twelve points from 0.5 to 20 cm was taken on the transverse plane with step sizes varying between 0.5 and 5 cm. Radial sampling did not occur in the outermost 5 cm of the phantom due to the inadequate amount of backscatter material at the phantom edge. Sampling off the transverse plane was taken in 1° polar angle increments. The source and resultant dose distribution were assumed to

be symmetric about the transverse plane, cylindrically symmetric about the source long axis, and azimuthal angle data were averaged. The $g_P(r)$ for total photon radiation was calculated from a weighted sum of primary and secondary ^{252}Cf photon radiation data. A multiplicative factor of 1.320×10^{10} s^{-1} mg^{-1} was applied to the primary radiation data and 2.314×10^{9} s^{-1} mg^{-1} to the secondary radiation data to account for the differential emission rate of ^{252}Cf primary photons with respect to secondary photons induced by spontaneous fission neutrons.

In this study, TG-43U1 brachytherapy dosimetry parameters computed for the hypothetical HDR ^{252}Cf source described above are determined and compared to similar data published for LDR ^{252}Cf applicator tube (AT) type sources. In addition, dosimetry parameters for common medical radionuclide sources are presented in contrast to the mixed-field behavior exhibited by HDR ^{252}Cf.

3 RESULTS AND DISCUSSION

Statistical uncertainties in F6 tallies of neutron dose on the transverse plane ranged from 0.1% to 0.4% from 0.5 to 20 cm, and 0.4% to 0.6% at the same distances for primary photon dose. Due to smaller solid angles, the statistical uncertainties increased for positions towards the source long axes. At 5°, the statistical uncertainties of neutron dose ranged from 0.3% to 1.2% from 0.5 to 20 cm, with values of 1.7% to 2.1% for photon dose at these same distances. Statistical uncertainties for photon transport were higher due to the lower density of energy deposition in the phantom, because the mean free path for photons ~ 1 MeV is longer than the average distance per neutron collision at the same energy.

3.1 Dosimetric Coefficients

For neutron transport simulations, comparison of F6 and F4 tallies provide an estimate of fluence-to-dose kerma coefficients, which are compared to values published in ICRU 63 in **Figure 3**. Similarly, the ratio of F6 and *F4 tallies for photon transport were taken to estimate mass-energy absorption coefficients, and are compared to coefficients published by NIST in **Figure 4** for 12 positions along the transverse axis.

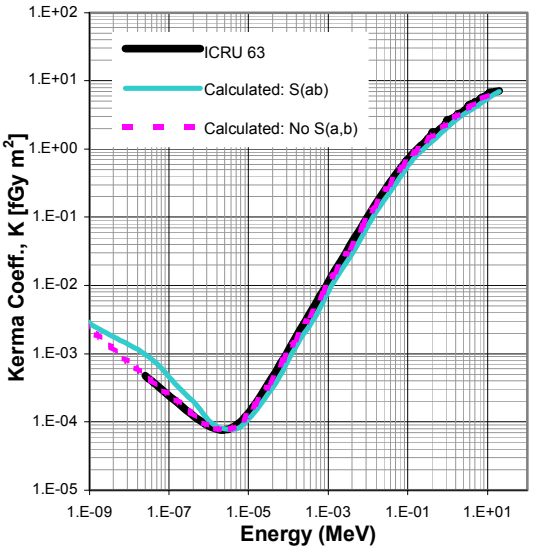

Figure 2: Comparison of neutron kerma coefficients published in ICRU 63 and those determined using MCNP5. The -calculated data is presented for simulations including and excluding the thermal neutron scattering factor S(α,β), which impacts energy deposition below 1 eV.

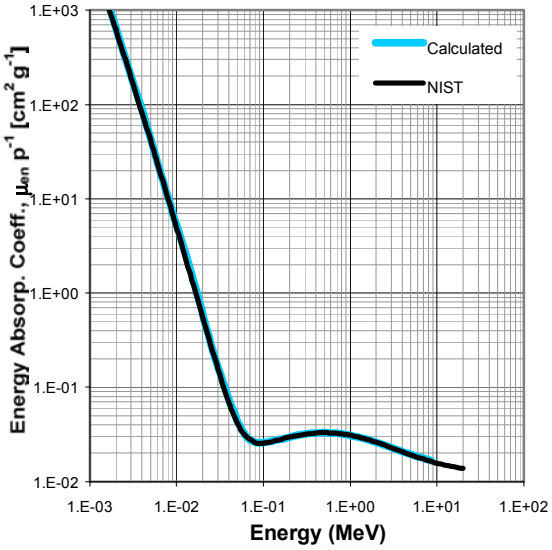

Figure 3: Comparison of photon energy-absorption coefficients calculated using MCNP5 and those published by NIST.

Neutron kerma coefficients calculated using MCNP5 are in good agreement with those published in ICRU Report 63 over seven decades of energy between 1 eV and 20 MeV. For thermal to low-energy neutrons (below 1 eV), there is a factor of 1.5 difference between this study and ICRU 63 for simulations employing the thermal neutron scattering factor S(α,β) for light water. Removal of S(α,β) results in better agreement to ICRU 63, with an average ratio of 0.98 ± 0.04 (± 1 s.d.) at 27 data points over nine orders of magnitude.

For photon energy deposition, a ratio of energy absorption coefficients calculated with MCNP5 and values published by NIST had an average of 1.01 ± 0.04 (± 1 s.d.) at 19 points over four decades. For photon energies below 0.1 MeV, MCNP5 calculated values were found to be sensitive to energy bin width as a result of rapid adsorption of low-energy photons.

3.2 Radial Dose Function g(r)

The HDR ^{252}Cf radial dose functions is shown in **Figure 4** for neutron radiation and in **Figure 5** for primary photon radiation. In **Figure 4**, $g_P(r)$ for ^{252}Cf neutrons is compared to similar data published by Rivard (2000) and by Yanch and Zamenhof (1992) for an AT type source (L = 1.5 cm). Radial dose function for primary photons displayed in **Figure 5** is compared to photon data calculated from Yanch and Zamenhof, to ^{192}Ir data published in TG-43, and to ^{125}I data for the Best Medical model 2031 seed published in TG-43U1.

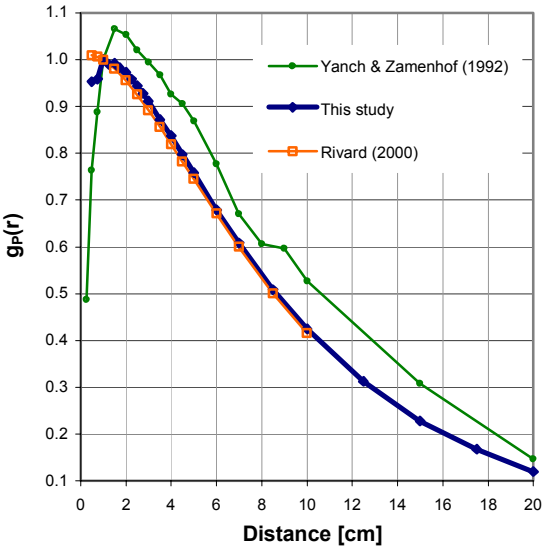

Figure 4: Radial dose functions for HDR ^{252}Cf neutrons compared to similar results for an AT type source published by Rivard (2000) and by Yanch and Zamenhof (1992).

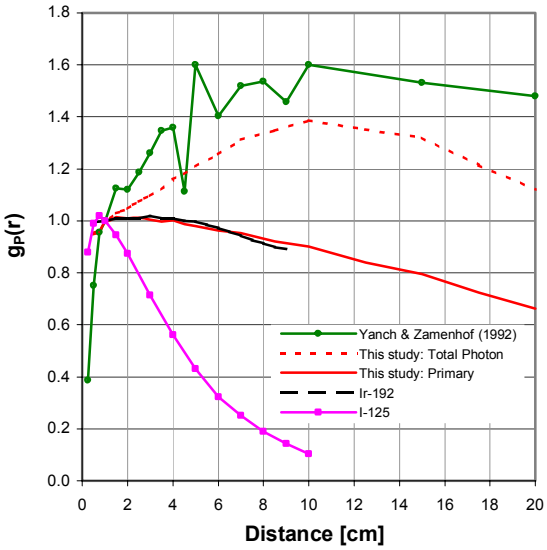

Figure 5: Radial dose function for ^{252}Cf photons in comparison to data published by Yanch and Zamenhof. In addition, $g_p(r)$ for two photon-emitting brachytherapy sources, the Best Medical model 2301 ^{125}I seed and a ^{192}Ir source, is shown.

Rivard determined the radial dose function using MCNP4B for a ^{252}Cf point source in a 30 cm water phantom assuming a Maxwellian neutron energy spectrum. Yanch and Zamenhof used MCNP3B to estimate $g_P(r)$ in water from an applicator tube (AT) type source in a cylinder of height 60 cm and radius 30 cm with a Watt fission spectrum representing the ^{252}Cf neutron emissions. Ratios of $g_P(r)$ to Rivard (2000) have an average value of 0.98 ± 0.03 (± 1 s.d.) between radial distances of 1 and 10 cm. Aside from utilizing a different neutron spectral model, differences in the neutron $g_P(r)$ data of Yanch and Zamenhof and this work are largely due to the neutron cross sections and kerma coefficients called by MCNP3B compared to the modern, up-to-date values in MCNP5. Further, Yanch and Zamenhof did not employ $S(\alpha,\beta)$ in their simulation to account for neutron moderation in liquid water. The discontinuity at $g_P(9)$ in the Yanch and Zamenhof data likely resulted from the precision of the data presented, and is not supported by the results of Rivard or this study.

Because secondary photons are induced outside of the source capsule, the total photon $g_P(r)$ builds to a maximum value at a depth of approximately 10 cm. The total photon radial dose function of Yanch and Zamenhof, calculated by subtracting the neutron dose from the total (neutron and photon) dose, exhibits similar behavior and supports the results of this study.

The low-energy radiations emitted by ^{125}I provide a steep radial dose function in contrast to ^{252}Cf neutrons and photons, due to the rapid attenuation of photons below 0.05 MeV in water. High energy photons from ^{192}Ir have an average energy of 0.37 MeV, and a $g_P(r)$ similar to that of ^{252}Cf primary photons. At a radial depth of 9 cm, $g_P(r)$ decreases only 10% for ^{252}Cf and ^{192}Ir photons, but there is a reduction of over 50% reduction for ^{252}Cf neutrons over the same distance.

Thus, the radial dose function behavior of radiation emitted by HDR ^{252}Cf is within the range of data presented for commonly applied medical radionuclides.

Calculation of $g_P(r)$ using the ^{252}Cf photon spectrum recommended by Knauer *et al*., which includes decay photons from fission products, was comparable to that determined using the primary photon emissions of Skarsvåg-Verbinski. Over all radial distances, a ratio of the two results had an average value of 0.98 ± 0.01 (± 1 s.d.). The ratios showed a slight increase with radial distance, such that the values were 0.99 and 0.97 at 2 and 20 cm, respectively.

3.3 2D Anisotropy Function F(r,θ)

Tables II and **III** displays the 2D anisotropy function data for neutron and photon radiation, respectively, for the HDR source shown in **Figure 1**. In **Table III**, the F6 tally results for primary and secondary photons were summed prior to calculating F(r,θ), as described above. Data are presented in 10° increments, representing the average of three degrees about each value, *e.g.*, the data for 50° is the average of 49°, 50°, and 51°. Because of the symmetry of the source, data equally spaced above and below the transverse plane was averaged to determine $F_{90}(r,\theta)$, *e.g.*, the data for 20° is the average of 20° and 160°.

Table II. 2D anisotropy functions for neutrons emitted from the HDR ^{252}Cf source.

	$F_{90}(r,\theta)$									
r (cm)	**0^0**	**10^0**	**20^0**	**30^0**	**40^0**	**50^0**	**60^0**	**70^0**	**80^0**	**90^0**
0.5	0.97	0.98	0.99	0.99	1.00	1.00	1.00	1.00	1.00	1.00
1.0	0.97	0.98	0.99	1.00	1.00	1.00	1.00	1.00	1.00	1.00
1.5	0.98	0.98	0.99	1.00	1.00	1.00	1.00	1.00	1.00	1.00
2.0	0.98	0.98	0.99	1.00	1.00	1.00	1.00	1.00	1.00	1.00
2.5	0.98	0.98	0.99	1.00	1.00	1.00	1.00	1.00	1.00	1.00
3.0	0.97	0.98	0.99	1.00	1.00	1.00	1.00	1.00	1.00	1.00
4.0	0.98	0.98	1.00	1.00	1.00	1.00	1.00	1.00	1.00	1.00
5.0	0.98	0.99	0.99	1.00	1.00	1.00	1.00	1.00	1.00	1.00
7.0	0.97	0.98	0.99	1.00	1.00	1.00	1.00	1.00	1.00	1.00
10.0	0.98	0.99	1.00	1.00	1.00	1.00	1.00	1.00	1.00	1.00
15.0	0.99	0.99	0.99	1.00	1.00	1.00	1.00	1.00	1.00	1.00
20.0	1.00	0.98	0.99	1.00	1.00	1.00	1.00	1.01	1.00	1.00

Table III. 2D anisotropy functions for primary and secondary (total) photon radiation emitted from the ^{252}Cf source.

	$F_{90}(r,\theta)$									
r (cm)	**0^0**	**10^0**	**20^0**	**30^0**	**40^0**	**50^0**	**60^0**	**70^0**	**80^0**	**90^0**
0.5	0.70	0.72	0.87	0.93	0.97	0.98	0.99	1.00	1.00	1.00
1.0	0.67	0.72	0.86	0.92	0.96	0.98	0.99	0.99	1.00	1.00
1.5	0.70	0.73	0.86	0.92	0.96	0.98	0.99	0.99	1.00	1.00
2.0	0.70	0.74	0.87	0.92	0.96	0.98	0.99	1.00	1.00	1.00
2.5	0.69	0.75	0.87	0.92	0.95	0.98	0.99	0.99	1.00	1.00
3.0	0.71	0.76	0.87	0.93	0.96	0.98	0.99	1.00	1.00	1.00
4.0	0.73	0.79	0.88	0.93	0.96	0.98	0.99	1.00	1.00	1.00
5.0	0.76	0.81	0.89	0.94	0.96	0.98	0.99	1.00	1.00	1.00
7.0	0.71	0.76	0.87	0.93	0.96	0.98	0.99	1.00	1.00	1.00
10.0	0.73	0.79	0.89	0.93	0.96	0.98	0.99	1.00	1.00	1.00
15.0	0.88	0.89	0.94	0.96	0.98	0.98	0.99	1.00	1.00	1.00
20.0	0.88	0.90	0.94	0.97	0.98	0.99	0.99	1.00	1.00	1.00

For both neutrons and photons, 99.9% of $F_{90}(r,\theta)$ data points were within 1% of the $F(r,\theta)$ for all radial distances and angles. For neutrons, 99% of the data were within ± 1% of the average value. For the photon data, adherence within ± 1% of the average values was 77% and increased to 98% for ± 5% agreement between $F_{90}(r,\theta)$ and $F(r,\theta)$.

Table III shows that anisotropy of the total photon emissions from a HDR ^{252}Cf source increases with decreasing θ and with decreasing radial distance, an effect that is exhibited by most photon-emitting brachytherapy sources described in TG-43U1. In contrast, 2D neutron dose deposition demonstrates only a 3% deviation along the source long-axis at a distance of 0.5 cm. This effect, attributed to the low rate of interaction between ^{252}Cf neutrons and the source encapsulation, was also noted by Rivard *et al.* and by Rivard.**[5,15]**

Impact of the choice of ^{252}Cf primary photon spectrum on $F_{90}(r,\theta)$ is shown in **Table IV** for selected radial distances. Over all distances, there was an average ratio of 1.04 ± 0.02 (± 1 s.d.) along the long axis ($\theta = 0^0$) and approaches unity towards the transverse plane with a standard deviation below 0.01 for 50^0, 60^0, 70^0, and 80^0.

Table IV. Ratio of the 2D anisotropy functions for ^{252}Cf primary photon emissions between the Knauer *et al.* and the Skarsvåg-Verbinski spectra. Data recommended by Knauer *et al.* includes estimates of the delayed photon intensity from the decay of ^{252}Cf fission products.

	$F_{90}(r,\theta)^{\text{Knauer } et\ al.} / F_{90}(r,\theta)^{\text{Skarsvåg-Verbinski}}$									
r (cm)	**0^0**	**10^0**	**20^0**	**30^0**	**40^0**	**50^0**	**60^0**	**70^0**	**80^0**	**90^0**
0.5	1.06	1.06	1.04	1.02	1.01	1.00	1.00	1.00	1.00	1.00
1.0	1.07	1.05	1.03	1.02	1.01	1.01	1.00	1.00	1.00	1.00
1.5	1.03	1.05	1.03	1.02	1.01	1.00	1.00	1.00	1.00	1.00
2.0	1.02	1.05	1.02	1.02	1.01	1.00	1.00	1.00	1.00	1.00
3.0	1.05	1.04	1.02	1.02	1.02	1.00	1.00	1.00	1.00	1.00
5.0	1.04	1.03	1.03	1.02	1.01	1.01	1.00	1.00	1.00	1.00
10.0	1.05	1.04	1.03	1.02	1.02	1.00	1.00	1.00	1.00	1.00
20.0	1.03	1.02	1.01	1.01	1.01	1.00	1.00	1.01	1.00	1.00

As such, utilization of the photon data of Knauer *et al.* will not significantly perturb the 2D anisotropy about the HDR ^{252}Cf source. The largest effects will occur towards the ends of the source at small radial distances. As expected, the 2D anisotropy function values using the photon energy spectrum from Knauer *et al*. were higher than the 2D anisotropy function values using the photon energy spectrum from Skarsvåg-Verbinski. This was due to the slightly higher average photon energy of Knauer *et al*. and increased path length through the capsule at oblique angles ($\theta \sim 0°$) along the source long-axis.

3.4 1D Anisotropy Function $\phi_{an}(r)$

1D anisotropy functions $\phi_{an}(r)$, calculated from the 2D anisotropy data in **Tables II** and **III**, are displayed in **Table V** for neutron and total photon radiations. For comparison, $\phi_{an}(r)$ for two photon emitting brachytherapy sources are included: the Best Medical model 2301 ^{125}I seed characterized in TG-43U1 and a high-energy ^{192}Ir source described in TG-43.

Table V. Comparison of 1D anisotropy functions between the neutron and photon emissions from a HDR ^{252}Cf source and two commonplace photon emitting medical sources. ^{192}Ir data was taken from TG-43, and ^{125}I data was the Best Medical model 2301 described in TG-43U1. Radial dose function $g_P(r)$ data are included for reference.

	$\phi_{an}(r)$				$g_p(r)$	
Radius (cm)	^{252}Cf Neutrons	^{252}Cf Photons	^{192}Ir Photons	^{125}I Photons	^{252}Cf Neutrons	^{252}Cf Photons
0.5	1.21	1.18			0.953	0.947
1.0	1.12	1.09	0.991	0.945	1.000	1.000
1.5	1.11	1.07			0.992	1.029
2.0	1.10	1.07	0.947	0.987	0.973	1.047
2.5	1.10	1.07			0.944	1.073
3.0	1.10	1.07	0.897	0.968	0.912	1.096
4.0	1.10	1.06	0.942	0.971	0.838	1.159
5.0	1.10	1.07	0.998	0.969	0.758	1.209
7.0	1.09	1.06	0.965	0.969	0.609	1.312
10.0	1.10	1.06			0.425	1.386
15.0	1.09	1.08			0.228	1.319
20.0	1.10	1.08			0.120	1.120

Compared to conventional photon-emitting brachytherapy sources, e.g., ^{192}Ir and ^{125}I, neutrons and photons from ^{252}Cf exhibit little change in their 1D anisotropy as a function of distance. Within 2 cm, both ^{252}Cf datasets show a steep increase in anisotropy approaching the source capsule.

4 SUMMARY

Radiation transport simulations were performed to evaluate the dosimetric characteristics of a simplified HDR ^{252}Cf brachytherapy source. Calculations performed to validate the MCNP5 F6 tally in comparison to the *F4 and F4 tallies typically indicated agreement of results with 2%. Subsequent simulations utilized models of ^{252}Cf neutron and photon emission to determine the 2D and 1D brachytherapy dosimetry parameters defined in the AAPM TG-43U1 report. The radial dose function for both neutrons and photons was consistent with previously published values, and within the range of variation exhibited by common medical radionuclide sources.

^{252}Cf neutron radiation exhibited little anisotropy about the plane-symmetric HDR capsule, and concomitant primary and secondary photons showed a general decrease in anisotropy with increasing radial distance, as expected due to scattered radiation. Further, evaluation of two separate ^{252}Cf primary photon spectra yielded comparable dosimetry parameters.

In conjunction, with an appropriate dose rate constant for this HDR ^{252}Cf source, data presented here may be incorporated into contemporary radiation therapy treatment planning systems towards clinical implementation and patient treatment.

5 ACKNOWLEDGMENTS

Support for one of the authors (CSM) was provided by appointment to the U.S. Department of Energy Nuclear Engineering and Health Physics Fellowship Program, sponsored by the U.S. Department of Energy's Office of Nuclear Energy, Science, and Technology.

6 REFERENCES

1. C. S. Schlea and D. H. Stoddard, "Californium isotopes proposed for intracavity and interstitial therapy with neutrons," *Nature,* **206**, pp. 1058-1059 (1965).
2. L. L. Anderson, "Status of dosimetry for ^{252}Cf medical neutron sources," *Physics in Medicine and Biology*, **6**, pp. 779-799 (1973).
3. J. C. Yanch and R. G. Zamenhof, "Dosimetry or ^{252}Cf sources for neutron radiotherapy with and without augmentation by boron neutron capture therapy," *Radiation Research*, **131**, pp. 249-25 (1992).
4. R. Nath, L. L. Anderson, G. Luxton, K. A. Weaver, J. F. Williamson, and A. S. Meigooni, "Dosimetry of interstitial brachytherapy sources: Recommendations of the AAPM Radiation Therapy Committee Task Group No. 43," *Medical Physics*, **22**, pp. 209-234 (1995).
5. M. J. Rivard, J. G. Wierzbicki, F. Van den Heuvel, R. C. Martin, and R. R. McMahon, "Clinical brachytherapy with neutron emitting ^{252}Cf sources and adherence to AAPM TG-43 dosimetry protocol," *Medical Physics*, **26**, pp. 87-96 (1999).
6. M. J. Rivard, B. M. Coursey, L. A. DeWerd, W. F. Hanson, M. S. Huq, G. S. Ibbott, M. G. Mitch, R. Nath, and J. F. Williamson, "Update of AAPM Task Group No. 43 Report: A revised AAPM protocol for brachytherapy dose calculation," *Medical Physics*, 31, pp. 633-674 (2004).
7. R. C. Martin, R. R. Laxson, J. H. Miller, J. G. Wierzbicki, M. J. Rivard, and D. L. Marsh, "Development of high-activity ^{252}Cf sources for neutron brachytherapy," *Applied Radiation Isotopes*, **48**, pp. 1567-1570 (1997).
8. X-5 Monte Carlo Team. MCNP – A general Monte Carlo N-Particle transport code, Version 5, Los Alamos National Laboratory, Los Alamos, NM (2003).
9. ICRU, "Nuclear data for neutron and proton radiotherapy and for radiation protection," *International Commission on Radiation Units and Measurements Report 63*, Bethesda, MD USA (2000).
10. J. H. Hubbell and S. M. Seltzer, "Tables of x-ray mass attenuation coefficients and mass energy-absorption coefficients (version 1.4)," National Institute of Standards and Technology, Gaithersburg, MD USA, http://physics.nist.gov/xaamdi (2005).
11. "Experimental Nuclear Reaction Data (EXFOR/CSISRS)," National Nuclear Data Center, Brookhaven National Laboratory, http://www.nndc.bnl.gov/exfor/index.html (2005).

12. W. Mannhart, "Evaluation of the Cf-252 fission neutron spectrum between 0 MeV and 20 MeV," *IAEA-TECDOC-410*, pp. 158-171 (1987).
13. V. V. Verbinski, H. Weber, and R. E. Sund, "Prompt gamma rays from ^{235}U(*n,f*), ^{239}Pu(*n,f*), and spontaneous fission of ^{252}Cf," *Physical Review C*, **7**, pp. 1173-1185 (1973).
14. K. Skarsvåg, "Differential angular distribution of prompt gamma rays from spontaneous fission of ^{252}Cf," *Physical Review C*, **22**, pp. 638-650 (1980).
15. J. B. Knauer, C. W. Alexander, and J. E. Bigelow, "Cf-252: properties, production, source fabrication and procurement," *Nuclear Science Applications*, **4**, pp. 3-17 (1991).
16. M. J. Rivard, "Neutron dosimetry for a general ^{252}Cf brachytherapy source," *Medical Physics*, **27**, pp. 2803-2815 (2000).
17. M. J. Rivard, C. S. Melhus, and B. L. Kirk, "Brachytherapy dosimetry parameters calculated for a new ^{103}Pd source," *Medical Physics*, **31**, pp. 2466-2470 (2004).